

DeltaCam: Differential Intrinsic Camera Modeling for Video Generation

DEBABRATA MANDAL, UNC, Chapel Hill, USA

ZHIHAN PENG, UNC, Chapel Hill, USA

YUJIE WANG, UNC, Chapel Hill, USA

PRANEETH CHAKRAVARTHULA, UNC, Chapel Hill, USA

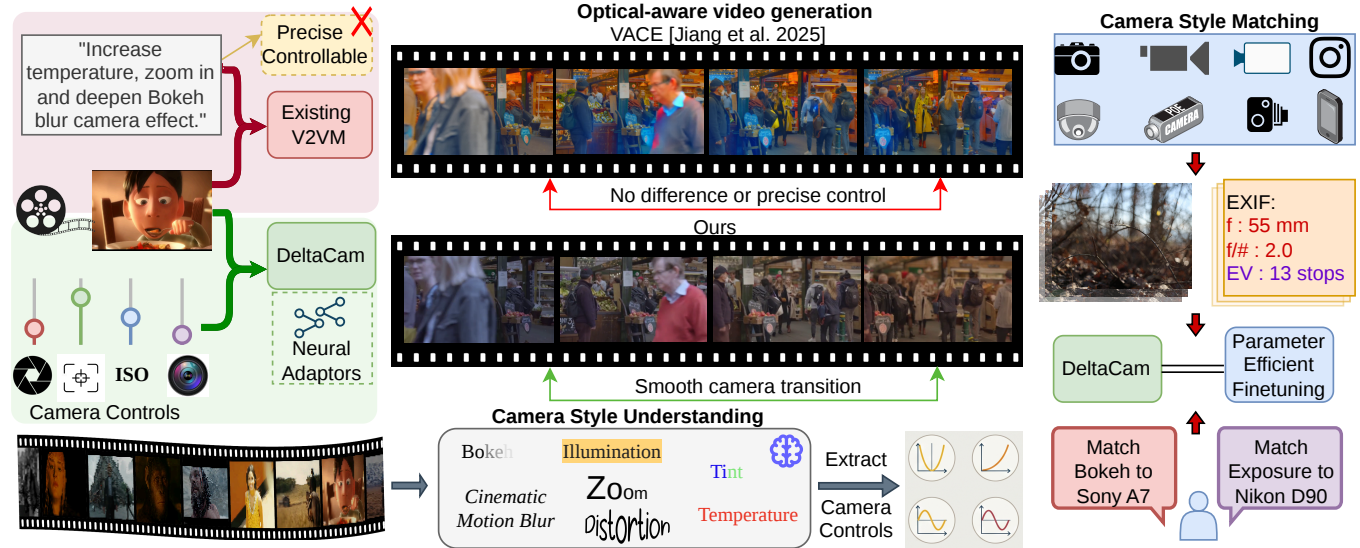


Fig. 1. Teaser figure. We present a fully integrated camera controlled video generation model including photographic and cinematographic effects such as *Bokeh* and *Dolly zoom*, while preserving original scene dynamics. Our method proposes a novel architectural block to disentangle camera conditioning for different parameters jointly during inference. Further, we also propose style extraction from videos for photographic concepts enabling video-to-video style transfer. Finally, we demonstrate our method can easily adapt its imaging process to diverse real camera types from just paired image camera EXIF metadata.

Incorporating camera intrinsics into video generation models offers a principled way to control not only scene dynamics but also the imaging process that governs visual appearance. Prior work has primarily focused on extrinsic control, such as camera pose and motion, while treating intrinsic camera parameters as implicit or fixed. A key bottleneck is the lack of large-scale video datasets with accurate and diverse temporally varying camera metadata, which makes learning absolute camera parameterizations difficult. As a result, current models struggle to incorporate photographic camera behavior, including depth-of-field transitions, exposure variations, lens distortions, and color processing, in a controllable and temporally consistent manner.

We introduce DeltaCam, a video diffusion framework that models camera behavior through Δ -parameterized neural camera adaptors, operating on relative changes in camera motion and intrinsics instead of absolute states. By learning this differential formulation from synthetic video data, we mitigate reliance on precise real-world camera labels and enable smooth, consistent control over imaging factors such as focal length, aperture, ISO, color temperature, and lens distortion. We extend this framework to real-world footage through two mechanisms: finetuning the controls on real image-metadata pairs for precise shot matching, and extracting disentangled embeddings for implicit video-to-video style transfer without requiring explicit camera parameters. By effectively separating scene content from intrinsic imaging behavior, DeltaCam enables camera-consistent video generation and editing operations that are difficult to achieve with existing models. Ultimately, our

results establish a practical and scalable approach for bridging synthetic control and real-world photographic emulation.

1 INTRODUCTION

Modern video generation models lack a principled and editable representation of camera behavior, a core component of real-world image formation and videography. In existing approaches [1, 32, 41], scene dynamics, camera motion, and camera intrinsics are all entangled within a single implicit latent space. While sufficient for casual video synthesis, this entanglement severely limits controllability and interpretability of camera behavior. In practice, this prevents fundamental operations like maintaining a consistent lens curvature across a generated shot or smoothly transitioning a camera parameter over time; the capabilities essential for real-world video creation and post-production editing. To verify this, we ran a simple experiment shown in Fig. 2 where we use text prompts, crafted with photography keywords to guide the video model generation. We find most state-of-the-art models fail to follow the user prompts accurately and sometimes even grossly deviating from the provided instructions. This limitation mainly stems from severe data constraints: large-scale video datasets rarely provide accurate, temporally consistent camera metadata, and camera intrinsics are often left fixed, unreliable, or not recorded at all. As a result, learning absolute camera parameterization is not only challenging but

Authors' addresses: Debabrata Mandal, debman@cs.unc.edu, UNC, Chapel Hill, USA; Zhihan Peng, UNC, Chapel Hill, USA, zp59@unc.edu; Yujie Wang, UNC, Chapel Hill, USA; Praneeth Chakravarthula, UNC, Chapel Hill, USA.

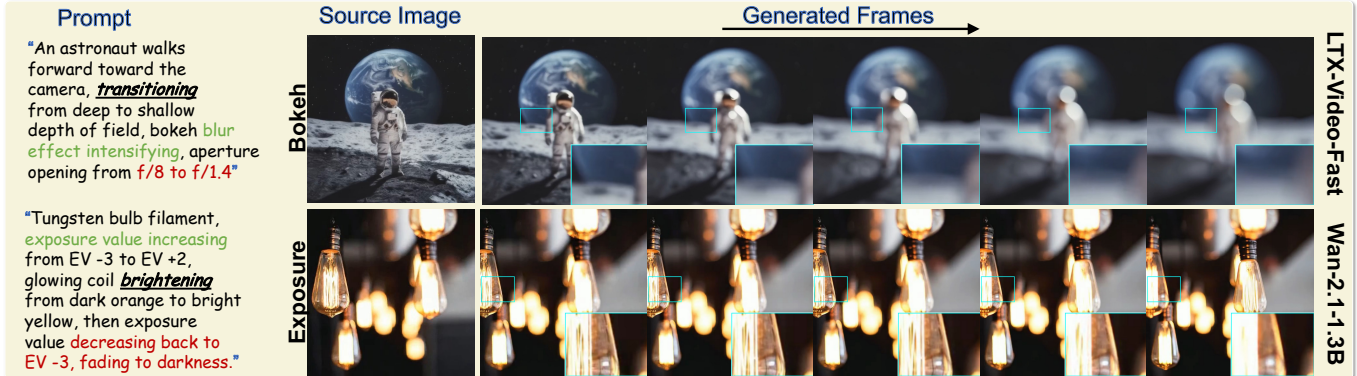


Fig. 2. *Limitations of current models.* We investigate the performance of prior text-to-video models [12, 30] with camera heavy text prompts to achieve accurate camera transitions. Text in green indicates prompt followed, while text in red represents prompt not followed.

also difficult to scale. Although most recent works have explored synthetic camera pipelines for controllable image generation [6, 38], these approaches do not extend naturally to temporally coherent video. Moreover, they often suffer from camera-parameter-image-appearance mismatches introduced by synthetic-to-real domain gap.

Here, we introduce *DeltaCam*, a video diffusion framework that models camera behavior through Δ -parameterized differential neural camera adaptors. Our framework is motivated by a key observation that cameras are *not* operated through absolute states, but through *relative changes*: adjusting zoom, aperture, exposure, or color settings gradually. We achieve this by varying a single camera parameter at a time during the video capture process in a smooth and continuous manner to mimic real world camera footage. Since the video backbone model’s core layers remain frozen, it implicitly learns to disentangle the photographic (camera intrinsic) concepts in the latent space. To better understand and control photographic concepts in video generation, we propose a disentangled camera control architecture where camera dynamics and scene information are controlled along different axes unlike prior works which do them jointly through spatial conditioning [38]. Furthermore, we extract temporally-varying camera style embeddings from videos disentangled from the scene content unlike prior works [20, 23].

Finally, we apply our camera style understanding and camera controlled video generation framework to applications such as video-to-video style transfer for photographic effects and camera style matching. Our contributions are summarized below,

- We *introduce* *DeltaCam*, a generative video framework that models camera behavior through Δ -parameterized differential neural adaptors, representing relative changes in camera motion and intrinsics.
- We *develop* a disentangled camera representation that separates camera extrinsics from intrinsics, while remaining robust to sparse and heterogeneous camera supervision.
- We *demonstrate* camera-consistent video synthesis and editing, enabling temporally smooth and transferable camera behavior that existing video generation models struggle to support.

- We further showcase several downstream applications using our model, including video-to-video style transfer and *parameter-efficient* camera style matching scalable to diverse new cameras.

2 RELATED WORK

As summarized in Table 1, prior work in generative camera control and optical modeling primarily focuses on geometric motion or image-level edits, leaving intrinsic camera behavior for video generation largely unaddressed.

2.1 Camera-Controlled Video Generation

Recent video generation works incorporate camera control primarily via extrinsics like viewpoint, pose, and trajectory [1, 2, 17, 41]. Training-based approaches inject explicit camera or geometry representations into diffusion models [4, 36]. These include ray-based embeddings (e.g., Plücker coordinates in AC3D [1] and SeVA [41]) and point-cloud renderings [35, 37]. ReCamMaster [2] trains a DiT on synthetic 4D data for cinematic transitions and refocusing. Conversely, training-free methods adapt pretrained models to novel trajectories. CamTrol [13] and LatentReframe [42] use point-cloud reprojection as geometric guidance for inpainting, while CamMiMic [10] transfers motion via homography-guided refinement without 3D reconstruction.

However, these methods treat camera control merely as geometric motion. Intrinsic imaging factors (focal length, aperture, ISO, color temperature, distortion) are absorbed into the video prior, limiting coherent synthesis of depth-of-field transitions, exposure ramps, white-balance shifts, and dolly zooms. *DeltaCam* addresses this by representing camera behavior as a temporally evolving control signal over both motion and intrinsic imaging parameters.

2.2 Camera-Intrinsic Control in Generative Models

Related works explore camera parameters and optical effects in generative image models. Early methods like NeuralCam [21] treat optical effects as image-to-image translation, learning separate modules for aperture, ISO, and noise. Recent text-to-image models introduce camera-aware conditioning: Generative Photography [38] and CamTokens [6] control focal length, aperture, and ISO, while PreciseCam [3] adds spatial control via ControlNet [39]. For video

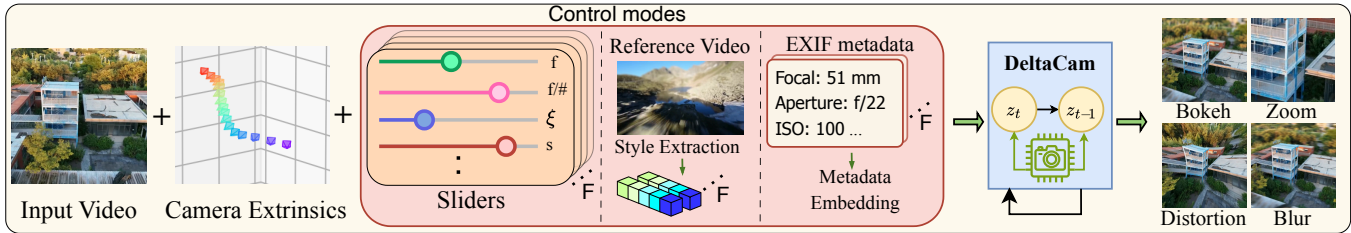


Fig. 3. Method Overview. We present a video-to-video generation pipeline with novel camera extrinsics and intrinsics controllable by *per-frame* sliders, a reference video with *photographic* styles, or real camera *paired* image-EXIF metadata.

Table 1. Comparison of related work on camera-controlled generation. Each criterion is fully ✓, partially (✓), or not met ✗. General Video-to-Video (V2V) editing models like VACE lack explicit, disentangled camera controls.

	GenPhoto [38]	AC3D [1]	Akira [32]	VACE [15]	ReCamMaster [2]	Ours
Model Characteristics						
Video-to-Video	✗	✗	✗	✓	✓	✓
Extrinsic Control	✗	✓	✓	✗	✓	✓
Intrinsic Control	✓	✗	✓	✗	✗	✓
Precise Control	✓	✗	✓	✗	✓	✓
Smooth Control	✗	✓	✓	✓	✓	✓
Style Mixing	✓	✗	✗	✗	✗	✓
Style Transfer	✗	✗	✗	✓	✗	✓
Camera Matching	✗	✗	✗	✗	✗	✓

generation, AkiRa [32] augments the standard pinhole camera model with aperture and lens-distortion modeling.

A parallel challenge is *representing* camera parameters to generalize across devices, sensors, and lenses. CamTokens [6] explores token embeddings for this; CCMNet [16] extracts camera-specific fingerprints for color constancy; and unified camera models aid perception tasks like depth estimation across diverse camera types [11]. Additionally, Puffin [18] introduces a camera-centric latent space for prompt-based scene guidance, albeit without explicit optical or photographic modeling.

While these methods establish camera parameters as generative controls, they typically map *absolute* camera states to visual effects. This requires precisely calibrated metadata—usually restricted to synthetic pipelines or curated still-image datasets—and ties mappings to specific sensor-lens combinations, limiting transfer to real video. Instead, DeltaCam maps *relative* camera changes to visual changes. This inductive bias is roughly device-invariant, enables supervision from sparse, heterogeneous real-world video, and naturally supports transferring camera trajectories between videos.

2.3 Cinematic Control and Video-to-Video Transfer

Fine-grained video generation control relies heavily on structured spatial and motion signals, including 3D bounding boxes [31], 2D poses [35], edge maps [40], motion cues [5], and point tracks [7], with extensions to long-form narratives [34] and motion recovery from blur [29]. While effective for scene layout and object motion, these handles leave camera-dependent imaging implicit: the temporal modulation of focus, exposure, or focal length—core cinematic behaviors—cannot be specified via spatial control maps.

Complementary works target *video-to-video transfer*, extracting reference attributes to re-apply to a target. SDEdit [19] established

training-free guided synthesis; VideoSwap [8] transfers subjects via 2D-keypoints, DDIM inversion [28], and latent blending; DreamVideo [33] fuses separately learned subject and motion adapters; and Diffusion-as-Shader [9] transfers motion using 3D point tracks. Recently, DisMo [25] extracted reusable motion representations disentangled from subject, appearance, and pose. While these methods successfully disentangle and transfer scene-level factors, none isolate the camera’s intrinsic imaging behavior.

Whereas prior works transfer object motion, identity, or style, we target this unexplored axis of camera behavior. Through reusable Δ -adapters, DeltaCam natively supports both a slider interface for direct parameter control and a reference-driven mode to extract and apply Δ -trajectories across videos for shot matching and camera-style transfer.

3 METHOD

This section details DeltaCam, our framework for integrating explicit, Δ -parameterized intrinsic camera control into video generation. We first introduce the core camera formulation and Camera Conditioning Module (CCM) in Sections 3.1 and 3.2, followed by our reference-style extraction and EXIF metadata matching techniques in Sections 3.3 and 3.4. The overall architecture is illustrated in Fig. 3, with the detailed CCM and multi-stage training curriculum (Section 3.5) depicted in Figs. 5 and 7.

3.1 Overview

We integrate a comprehensive, general (non-pinhole) camera model into the video generation pipeline, operable via three main control modes: *parameter sliders*, *style embeddings*, and *EXIF metadata embeddings* (Fig. 3). Our primary focus is video-to-video generation guided by camera-centric controls that explicitly decouple camera trajectory (extrinsics) from photographic effects (intrinsic).

Unlike standard pinhole models typically assumed in rendering pipelines, real cameras introduce complex optical and sensory transformations. We model this capture process as a function Φ governed by the underlying 3D scene S , extrinsic pose $P \in SE(3)$, and a K -dimensional vector of intrinsic photographic parameters $\theta \in \mathbb{R}^K$ (e.g., focal length, aperture, ISO):

$$I = \Phi(S, P, \theta) \quad (1)$$

Inverting Eq. (1) to estimate these intrinsic parameters from raw video is highly ill-posed. However, solving this inverse problem is essential for enabling video-to-video camera style transfer when explicit metadata is unavailable.

The following subsections detail our approach for conditioning the video generative model for full camera-aware synthesis, extracting these camera styles directly from reference footage, and validating the model’s generalization by matching the shot profile of real-world cameras using paired image-EXIF data.

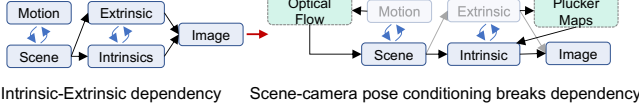


Fig. 4. Camera conditioning circular dependency. Real videos are captured in dynamic environments with moving objects or moving camera leading to a criss-cross dependency in the final imaging process. For video generation, we break this circular dependency by conditioning the model on optical flow and per-frame camera extrinsic for generating the video along a different camera trajectory.

3.2 Camera video conditioning

Architecture Motivation. The camera capture process in Eq. (1) mixes any change in scene, extrinsics, or intrinsics in any order (Fig. 4). We break this entanglement by anchoring scene content via the source video and conditioning generation on geometric proxies G (depth, optical flow, and perspective fields) to serve as the spatial backbone, helping the model identify structure, motion, and orientation. To ensure consistent viewpoint rendering, we encode the new extrinsic camera pose (relative to starting frame) P as spatial Plücker ray maps [27] and inject them into both the intrinsic conditioning branch and the base video diffusion model. We zero out the pose ray maps in the case of same video camera style editing (no novel view) and keep this behavior consistent during inference. The proxy maps G provide additional 3D scene cues over the RGB video.

Accordingly, we design our Camera Conditioning Module (CCM) to modulate these 3D spatial cues based on user-defined photographic trajectories (Fig. 5). However, absolute camera parameters are ambiguous without knowing the camera type, which alters how each parameter maps to the final appearance. We therefore adopt a Δ -parameterization: given an intrinsic trajectory, we define the relative control at time t with respect to the anchor frame as $\Delta\theta_t = (\theta_t - \theta_1)/r$, where r is the parameter’s maximum range. This (a) decouples training from the specific camera, since a Δ directly maps to a change in effect, and (b) cleanly isolates individual effects (e.g., Bokeh, zooming) by varying one $\Delta\theta_i$ while holding the rest at zero (i.e., locked to the anchor frame).

The spatial proxy maps G_t are first compressed into latent features h_t via a frozen 3D VAE encoder. We then modulate these spatial features using Feature-wise Linear Modulation (FiLM) [22] driven by the relative intrinsics:

$$\text{FiLM}(h_t, \Delta\theta_t) = \gamma(\Delta\theta_t) \odot h_t + \beta(\Delta\theta_t), \quad (2)$$

where γ and β are scaling and shifting tensors predicted by a multi-layer perceptron (MLP) from the relative control input $\Delta\theta_t$. These FiLM layers use simple affine transformations to adjust the optical style globally. Because they preserve the underlying scene structure, they naturally encourage the model to disentangle camera effects from scene content in the latent space. We split the intrinsics into optical, sensory, and ISP groups, each routed through a separate FiLM

cascade (Fig. 5). Cascading these FiLM layers across the encoded spatial feature maps aggregates the final intrinsic conditioning before fusing it with the base video latent representation z_t .

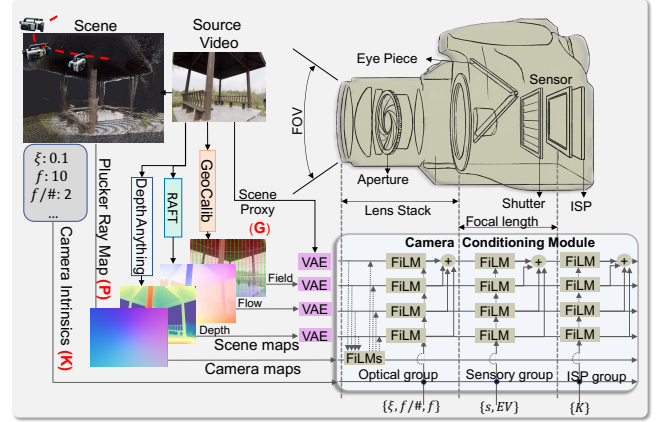


Fig. 5. Camera Conditioning Module. Our proxy camera model works by disentangling the optical, sensory and image characteristics (K) of regular hand held cameras. Scene maps (G) such as depth, optical flow and perspective fields are used to guide the video generation process from our camera model as a substitute for the real 3D world.

3.3 Reference Camera Style Extraction

We extract reusable camera style embeddings from videos by explicitly disentangling spatial representations into orthogonal content and style branches (Fig. 6). To supervise this disentanglement, we construct training batches comprised of synthetic video triplets (x_a, x_c, x_s) generated via our synthetic camera pipeline. This synthetic environment is crucial, as it allows us to perfectly isolate variables that are otherwise impossible to decouple in real-world footage. Specifically, the anchor video x_a shares the exact scene content with x_c but under a different camera trajectory, while x_s shares the exact camera trajectory with x_a but depicts an entirely different scene:

$$x_a \xrightarrow{\text{same scene}} x_c, \quad x_a \xrightarrow{\text{same style}} x_s. \quad (3)$$

We extract spatial patch features from each clip with a frozen c -RADIO ViT-H backbone[24], and subsequently aggregate them using a lightweight temporal transformer. The network then bifurcates to decode a scene content embedding z_c and a per-frame style embedding z_s . A dedicated regression head maps z_s to the predicted intrinsic trajectory $\hat{\tau}$ (representing the temporal evolution of our camera parameters).

This structure drives the disentanglement objective: the content branch is trained to maximize the similarity between the content embeddings of (x_a, x_c), while the style branch aligns the style embeddings of (x_a, x_s). The overall style extraction loss function is:

$$\mathcal{L} = \lambda_\tau \mathcal{L}_{\text{NCC}}(\hat{\tau}, \tau) + \lambda_c \mathcal{L}_{\text{NCE}}(z_c^a, z_c^c) + \lambda_s \mathcal{L}_{\text{NCE}}(z_s^a, z_s^s) + \lambda_{\text{MI}} \mathcal{L}_{\text{MI}}(z_c, z_s) \quad (4)$$

where \mathcal{L}_{NCC} measures trajectory prediction accuracy via Normalized Cross-Correlation against the ground truth trajectory τ , and \mathcal{L}_{NCE} is the standard InfoNCE contrastive loss term [23]. To explicitly penalize residual dependence between the content and style branches, \mathcal{L}_{MI} minimizes the squared cosine similarity between

content and style embeddings. To populate this training data, we leverage our synthetic camera pipeline to sample diverse trajectories across commonly used photographic effects, including *Bokeh*, dolly zooms, lens curvature, exposure ramps, cinematic blur, and color temperature.

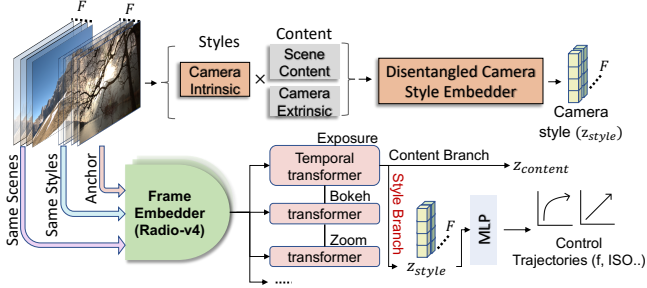


Fig. 6. Camera Style Extraction. Our camera style embedder extracts styles from video by differentiating between the content and styles from a batch of videos. The styles are extracted on a per-frame basis for each common photographic effects (e.g. Bokeh, zooming) using a shared temporal transformer. The final styles are projected into 1D camera parameters (e.g. f , aperture) by linear MLP layers.

3.4 Camera Style Matching

While DeltaCam relies on relative Δ -parameterization learned from synthetic data, practical applications often require grounding the model to absolute, real-world camera states. We achieve this through *Camera Style Matching*, which adapts our synthetic-trained controls using real image-metadata pairs for precise, camera-specific shot emulation.

Given a vector of absolute per-frame parameters $\mathbf{m}_t \in \mathbb{R}^{N_{\text{meta}}}$ derived from image EXIF metadata (e.g., aperture f , focal length ℓ , ISO speed s), we first map each physical quantity to a normalized scalar to reflect perceptual linearity (where equal steps correspond to equal perceptual increments, such as one f-stop or one EV). We define the normalized vector $\tilde{\mathbf{m}}_t \in [0, 1]^{N_{\text{meta}}}$ via a log-space mapping for each element i :

$$\tilde{m}_{t,i} = \frac{\log(m_{t,i}/m_{\min,i})}{\log(m_{\max,i}/m_{\min,i})} \quad (5)$$

A lightweight EXIF metadata tokenizer $\Phi_{\text{meta}} : \mathbb{R}^{N_{\text{meta}}} \rightarrow \mathbb{R}^{d_{\xi}}$ implemented as a two-layer MLP with a SiLU activation and a zero-initialized output layer—maps this normalized state to a latent style embedding $\xi_t = \Phi_{\text{meta}}(\tilde{\mathbf{m}}_t)$. This generates a continuous per-clip metadata sequence $\xi \in \mathbb{R}^{T \times d_{\xi}}$ that integrates directly into our conditioning pipeline.

3.5 Training Curriculum

We employ a three-stage curriculum to align the base Video Diffusion Model (VDM) with our camera-aware framework without degrading its innate generative priors (Fig. 7):

(1) *Base pre-training*: We train the Camera Conditioning Module (CCM) and a set of new, independent self-attention blocks using synthetic data. To preserve the base VDM’s high-quality video generation, we leave all of its original layers completely frozen. The model processes the extrinsic pose \mathbf{P} and relative intrinsic trajectories $\Delta\theta_t$ by concatenating them with the video latent z_t and passing them exclusively through the new attention blocks.

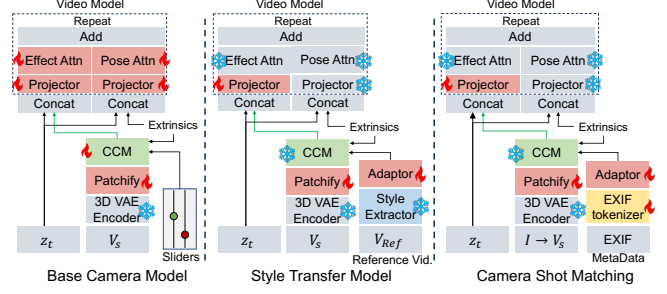


Fig. 7. Camera-VDM integration. We condition the VDM on camera extrinsics and intrinsics (through CCM) separately from one another. Style transfer and camera style matching are achieved through lightweight adaptors added prior to the camera encoder (CCM).

- (2) *Style transfer adaptation*: We freeze the VDM, the core CCM, and the new attention blocks. We then train only lightweight style extractor, teaching it to map reference embeddings extracted trajectory into the prior learnt Δ -parameter control space.
- (3) *Real-world matching*: We keep the entire network (from stage 1) frozen and train only the EXIF metadata tokenizer Φ_{meta} . This step translates the absolute normalized sequence ξ_t into our synthetic control space, allowing the model to accurately emulate real cameras. Real world camera adaptation requires updating less than 0.1% of the overall model parameters allowing *parameter efficient finetuning* of the diffusion model to diverse camera types.

Extended architectural details are provided in the supplementary.

4 EXPERIMENTS

4.1 Dataset & Implementation

We train on a 50:50 mix of RealCamVid [17] (single-camera real-world videos) and MultiCam [2] (synthetic multi-camera scenes) for stages 1 & 2, covering both extrinsic and intrinsic control. Stage 3 uses EXIF-paired image datasets: RealBokeh [26] (bokeh) and NeuralCam [21] (exposure).

We build on Wan-2.1 (1.3B) [30] at 480×832 resolution. We use Adam ($\text{lr} = 10^{-5}$), 50 denoising steps, and train on a single RTX A6000 (96GB) for 60K/15K/6K iterations across the three stages.

4.2 Evaluation

Baseline models. We compare our camera-controlled VDM and provide quantitative metrics against prior works such as VACE-1.3B [15] and CogVideoX-5B-V2V [36] both of which support text prompted video-to-video generation based on a diffusion transformer backbone.

Metrics. We report reference-based fidelity (PSNR, SSIM, LPIPS) against synthetic ground-truth videos, and general video quality and temporal smoothness using VBench [14]. Because these metrics evaluate high-level features and lack sensitivity to fine-grained optical effects, we introduce a targeted metric, wCLIP-5.

wCLIP-5 (Windowed CLIP Similarity). To accommodate minor temporal jitter without allowing semantic divergence, we compute a windowed cosine similarity over a ± 2 frame neighborhood. Let $\mathcal{E}_{\text{CLIP}}(\cdot)$ denote the CLIP image encoder; given generated frames

$\{\hat{\mathbf{x}}_t\}_{t=1}^T$ and reference frames $\{\mathbf{x}_t\}_{t=1}^T$,

$$\text{wCLIP-5} = \frac{1}{T} \sum_{t=1}^T \max_{k \in \{-2, \dots, 2\}} \cos(\mathcal{E}_{\text{CLIP}}(\hat{\mathbf{x}}_t), \mathcal{E}_{\text{CLIP}}(\mathbf{x}_{t+k})), \quad (6)$$

where out-of-bounds indices are ignored. The ± 2 window relaxes strict temporal alignment, so gains on this metric reflect semantic rather than phase alignment.

4.3 Results

We systematically evaluate DeltaCam’s ability to render precise camera effects, mix multiple parameters, and extract reusable styles from reference footage.

4.3.1 Single-Effect Camera Control. We first evaluate the precision of DeltaCam in rendering isolated photographic effects against state-of-the-art text-to-video baselines, VACE and CogVideoX. As qualitatively shown in Fig. 8, our method accurately matches the synthetic ground truth trajectories for effects such as bokeh, exposure, and zooming. In contrast, text-prompted baselines struggle to render these physical transitions smoothly, often ignoring the prompt or hallucinating scene changes.

Quantitatively (Table 2), DeltaCam achieves the strongest fidelity on average—improving PSNR by 3.1 dB and LPIPS by 0.12 over the next-best baseline, while maintaining comparable VBench temporal scores. Per-effect, DeltaCam leads on five of six categories across PSNR, SSIM, and LPIPS, with the largest margins on photometric effects (Color Temp. +4.2 dB, Exp. Time +5.0 dB). For *geometric* effects (lens distortion, focal length, motion blur), reference-based metrics like PSNR and LPIPS are inherently less discriminative: small spatial displacements between rendered and ground-truth frames are penalized at full strength even when the underlying effect is faithfully reproduced. The wCLIP-5 metric, which operates on semantic features within a temporal window, better isolates effect

Table 2. Quantitative comparison across different camera control effects. We evaluate across three categories of metrics: reference metrics such as PSNR and LPIPS, general video quality metrics such as VBench, and our temporal similarity metric wCLIP-5.

Effect / Method		Reference Metrics			VBench		Sim.
		PSNR \uparrow	SSIM \uparrow	LPIPS \downarrow	Temp. \uparrow	Smooth \uparrow	wCLIP-5 \uparrow
Bokeh	VACE	19.86	0.74	0.36	0.97	0.98	0.89
	CogVideoX	21.27	0.68	0.32	0.96	0.99	0.92
	Ours	25.21	0.79	0.29	0.97	0.98	0.94
Motion Blur	VACE	20.49	0.73	0.41	0.97	0.98	0.89
	CogVideoX	21.70	0.72	0.33	0.96	0.99	0.92
	Ours	20.82	0.74	0.31	0.97	0.99	0.94
Lens Dist.	VACE	11.55	0.37	0.69	0.97	0.98	0.83
	CogVideoX	12.27	0.40	0.62	0.96	0.98	0.88
	Ours	13.92	0.44	0.49	0.98	0.98	0.91
Exp. Time	VACE	15.35	0.75	0.30	0.98	0.98	0.90
	CogVideoX	16.14	0.65	0.29	0.96	0.99	0.94
	Ours	21.08	0.74	0.22	0.97	0.98	0.96
Color Temp.	VACE	12.42	0.55	0.50	0.98	0.99	0.84
	CogVideoX	19.30	0.71	0.26	0.97	0.99	0.95
	Ours	23.51	0.90	0.11	0.98	0.98	0.98
Focal Len.	VACE	11.14	0.40	0.67	0.97	0.98	0.84
	CogVideoX	11.61	0.43	0.62	0.96	0.99	0.87
	Ours	16.51	0.55	0.33	0.96	0.98	0.96
Average	VACE	15.13	0.59	0.49	0.97	0.98	0.87
	CogVideoX	17.05	0.60	0.41	0.96	0.99	0.91
	Ours	20.18	0.69	0.29	0.97	0.98	0.95

Table 3. Per-effect style extraction performance. NCC measures trajectory prediction accuracy (higher is better); Style InfoNCE measures scene independence (lower is better; random ceiling ≈ 4.07); Valid fraction is the proportion of evaluation samples in which the ground-truth camera parameter varies over time (GT std $> 10^{-3}$), i.e., the fraction for which NCC is defined during training. Baselines use c-RADIO v4: B1: NCC-only loss, w/o temporal encoder. B2: NCC-only loss, w/ temporal encoder.

Effect	Param.	B1 NCC \uparrow	B2 NCC \uparrow	Ours NCC \uparrow	Style (ours) InfoNCE \downarrow	Valid Frac. \uparrow
Focal length	F	0.32	0.75	0.84	0.38	0.90
Lens distortion	ξ	0.22	0.25	0.45	0.47	1.00
Bokeh	Aperture	0.27	0.35	0.82	2.84	0.76
	Focus dist.	0.13	0.20	0.43		0.82
Exposure	EV	0.77	0.80	0.89	0.03	0.80
Motion blur	Shutter	0.09	0.25	0.61	2.93	0.93
Color temp.	Color temp.	0.78	0.83	0.90	0.03	0.79

fidelity in these cases and shows DeltaCam consistently leading (e.g., 0.91 vs. 0.88 on lens distortion; 0.96 vs. 0.87 on focal length). Matched VBench scores further confirm that injecting explicit Δ -parameterized control preserves the base model’s inherent temporal consistency and spatial smoothness.

4.3.2 Full Camera Control and Style Mixing. Beyond isolated parameters, real-world cinematography requires the joint manipulation of multiple variables. In Fig. 9, we demonstrate full camera control by applying four distinct extrinsic camera trajectories, each coupled with a different combination of intrinsic effects, to a single source video. DeltaCam successfully disentangles these signals, generating temporally consistent novel views while simultaneously applying the requested optical shifts. We further push this capability in Fig. 12, demonstrating complex style mixing where two distinct photographic parameters (e.g., focal length and color temperature, or bokeh and exposure) are smoothly modulated at the same time without mutual interference or degradation of the underlying scene dynamics.

4.3.3 Camera Style Extraction. To evaluate reference-driven capabilities, we test our model’s ability to invert camera effects from existing footage without explicit metadata. Fig. 11 visualizes the accuracy of our style extraction module: we extract the intrinsic trajectory from a reference video and re-apply it to its original source frame. As highlighted by the detailed insets, DeltaCam faithfully reconstructs the temporal evolution of the reference’s optical style.

Quantitatively (Table 3), our network achieves high Normalized Cross-Correlation (NCC) for photometric effects like color temperature (0.90) and exposure (0.89), with near-perfect scene disentanglement (Style InfoNCE ≈ 0.03). We compare against two c-RADIO v4 baselines that use only the NCC trajectory loss: B1 (per-frame) and B2 (with our temporal encoder). Our full method outperforms both across every effect, with the largest gains on geometric and spatially coupled effects (focal length 0.32/0.75 \rightarrow 0.84, aperture 0.27/0.35 \rightarrow 0.82, motion blur 0.09/0.25 \rightarrow 0.61). The small B1 \rightarrow B2 gap relative to the larger B2 \rightarrow Ours gap confirms that our disentanglement objectives—not architecture alone— isolate the camera signal from scene content.

For spatially dependent effects like Bokeh and motion blur, trajectory prediction remains strong (aperture NCC 0.82) but Style

InfoNCE only partially decreases from the random ceiling (2.84 and 2.93 vs. 4.07). This is expected: defocus and motion blur are physically coupled to scene depth and object velocity, so perfect content/style separation is fundamentally limited rather than a model failure. The trajectory head nonetheless decodes the parameter curve accurately, indicating that z_{style} encodes the right signal even when not fully scene-orthogonal. The practical implication for inference is that z_{style} can act as a “leaky” embedding for spatially coupled effects: when transferring bokeh from a reference video, the embedding may carry residual appearance traits from the source scene. This leakage is generally tolerable for structural effects like aperture and focus, and is largely avoided for photometric effects in isolation; cross-group leakage is discussed in the supplementary.

4.3.4 Applications. We demonstrate two practical use cases. **Real camera shot matching** (Fig. 10): grounding DeltaCam to specific cameras (Sony A7, Nikon Z6, Canon R6) via the EXIF tokenizer not only provides absolute parameter control but also improves perceptual quality leading to more natural Bokeh falloff and better exposure dynamic range, whereas the synthetic-trained base model shows visible artifacts. Critically, this adapts to new cameras with <0.1% additional parameters, no backbone retraining. **Video-to-video style transfer** (Fig. 14): the style extractor infers an effect trajectory from a reference video and re-applies it to a different source, transferring photographic intent (e.g., a cinematic bokeh ramp) without specifying explicit parameters. Together these span the practical spectrum from precise numerical to intuitive reference-driven control.

4.4 Ablation Studies

Table 4 reports results for three design choices. Zeroing individual 2D proxy streams produces minor changes (≤ 0.15 dB PSNR, ≤ 0.004 LPIPS), with source RGB causing the only measurable perceptual shift (LPIPS 0.208 vs. 0.204). This indicates the model treats the proxy streams as redundant geometric cues rather than relying on any single one, with RGB carrying the dominant appearance signal. Replacing the Δ -parameterization with unnormalized *absolute* parameters collapses performance dramatically (23.29 \rightarrow 11.88 dB PSNR; SSIM 0.962 \rightarrow 0.360), as the model fails to map absolute camera parameters to the scene state at starting frame. Finally, simultaneous Bokeh+Exposure conditioning achieves 21.57 dB, within ~ 1.4 dB of single-effect baselines (22.94 and 20.35 dB), with the small gap absorbed on the harder single effect (Exposure). This shows the group-disentangled FiLM architecture handles multi-effect inputs with minimal interference.

4.5 Limitations

DeltaCam’s disentanglement relies on the accuracy of deterministic spatial proxies (e.g., optical flow and monocular depth). In extreme scenarios, where these estimators fail (Fig. 13), such as scenes with heavy motion blur, severe occlusions, or complex transparent surfaces—the conditioning module may propagate geometric artifacts into the final generation. Additionally, we restrict experiments to a 1.3B backbone (Wan-2.1) for compute reasons; scaling to larger backbones and longer video sequences is left to future work.

Table 4. Ablation study on DeltaCam. Metrics averaged over all effects.

(a) Component ablation performed over an ablation split separate from Table 2.

Variant	PSNR \uparrow	SSIM \uparrow	LPIPS \downarrow
<i>Proxy Stream Contribution (stream-zeroing)</i>			
Full model (all streams)	22.65	0.875	0.204
w/o Depth stream	22.50	0.875	0.201
w/o Optical flow	22.68	0.876	0.201
w/o Perspective field	22.63	0.875	0.202
w/o Source RGB	22.63	0.873	0.208
w/o All 2D streams	22.47	0.876	0.200
<i>Absolute vs Delta Parameterization</i>			
Absolute (w/o range normalization)	11.88	0.360	0.738
Delta (w/ normalization)	23.29	0.962	0.103
<i>Multi-Effect vs. Single-Effect Conditioning</i>			
Single: Bokeh only	22.94	0.859	0.291
Single: Exposure only	20.35	0.949	0.136
Multi: Bokeh + Exposure	21.57	0.854	0.274

(b) wCLIP temporal window sensitivity.

Method	wCLIP-1 \uparrow	wCLIP-5 \uparrow	wCLIP-10 \uparrow
VACE	0.85	0.87	0.87
CogVideoX	0.89	0.91	0.92
Ours	0.94	0.95	0.95

5 CONCLUSION

We present DeltaCam, a video generation framework enabling explicit, temporally consistent control over intrinsic photographic effects. By leveraging a novel Δ -parameterized control space and a three-stage training curriculum, our approach overcomes the severe data scarcity of real-world camera-paired videos. DeltaCam supports fine-grained optical control (e.g., bokeh, exposure ramps, dolly zooms), reference-driven style extraction, and precise real-world shot matching. Extensive evaluations demonstrate that DeltaCam significantly outperforms existing text-driven baselines in rendering accurate, disentangled camera intrinsics. Ultimately, this work establishes a scalable foundation for decoupling scene content from optical imaging behavior, advancing the capabilities of professional-grade generative cinematography.

ACKNOWLEDGMENTS

We are grateful to UNC Research Computing for providing access to the Longleaf cluster, on which the experiments in this work were conducted.

REFERENCES

- [1] Sherwin Bahmani, Ivan Skorokhodov, Guocheng Qian, Aliaksandr Siarohin, Willi Menapace, Andrea Tagliasacchi, David B Lindell, and Sergey Tulyakov. 2025. Ac3d: Analyzing and improving 3d camera control in video diffusion transformers. In *Proceedings of the Computer Vision and Pattern Recognition Conference*. 22875–22889.
- [2] Jianhong Bai, Menghan Xia, Xiao Fu, Xintao Wang, Lianrui Mu, Jinwen Cao, Zuozhu Liu, Haoji Hu, Xiang Bai, Pengfei Wan, et al. 2025. Recammaster: Camera-controlled generative rendering from a single video. *arXiv preprint arXiv:2503.11647* (2025).
- [3] Edurne Bernal-Berdun, Ana Serrano, Belen Masia, Matheus Gadelha, Yannick Hold-Geoffroy, Xin Sun, and Diego Gutierrez. 2025. PreciseCam: Precise Camera Control for Text-to-Image Generation. In *Proceedings of the Computer Vision and Pattern Recognition Conference*. 2724–2733.

- Mandal et al.



Fig. 8. Visual Comparisons. We evaluate our camera controlled generation model on several complex photographic arcs against prior state-of-the-art works.



Fig. 9. Full camera control. By separating the intrinsic conditioning from extrinsic conditioning we achieve novel view generation by specifying novel camera pose trajectories while also simultaneously controlling photographic concepts as well.

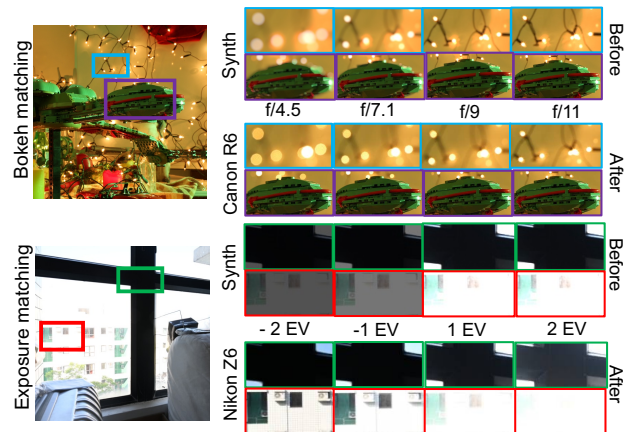


Fig. 10. Real Camera Shot Matching. Our camera matching step (Bokeh → RealBokeh; exposure → NeuralCam) matches the shot profile for camera effects from real camera paired EXIF captures making it realistic.

[4] Andreas Blattmann, Tim Dockhorn, Sumith Kulal, Daniel Mendelvitich, Maciej Kilian, Dominik Lorenz, Yam Levi, Zion English, Vikram Voleti, Adam Letts, et al.

2023. Stable video diffusion: Scaling latent video diffusion models to large datasets. *arXiv preprint arXiv:2311.15127* (2023).

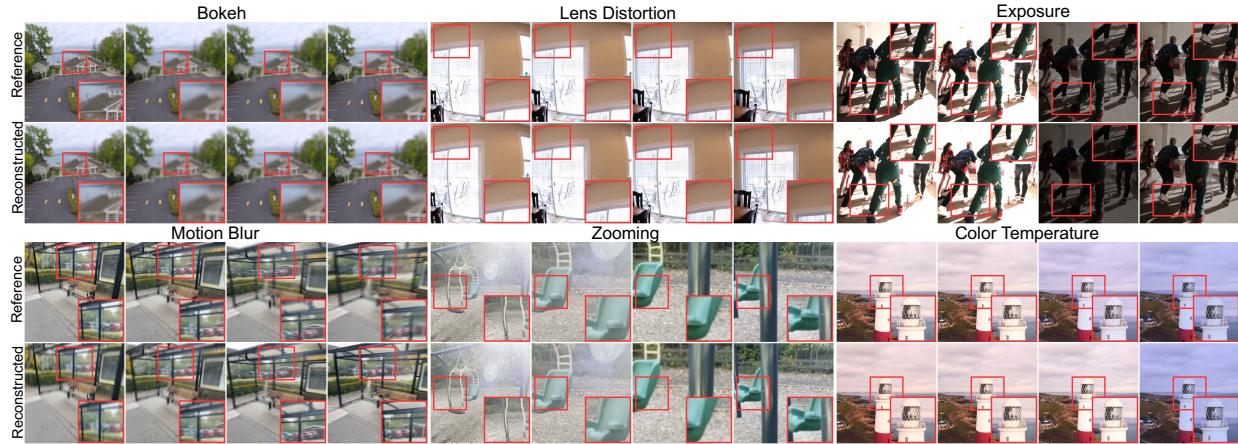


Fig. 11. Camera style extraction. We show styles extracted from video frames across timestep with photographic styles re-applied on the source video to check consistency. Our model consistently follows the style trajectory in the reference video across multiple timestamps for every effect.

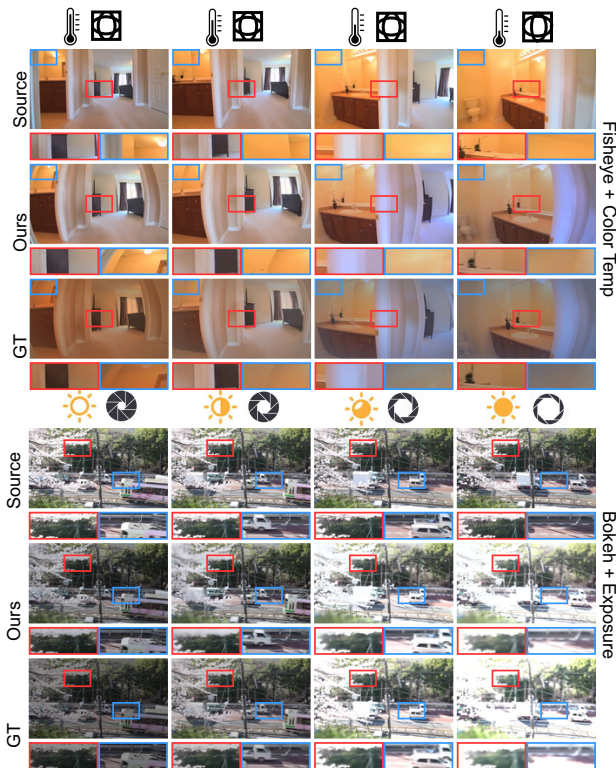


Fig. 12. Style mixing. Joint camera control of several photographic effects as a result of the latent disentanglement process employed during model training.

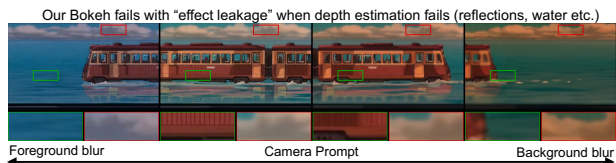


Fig. 13. Limitations. Inaccurately estimated spatial cues affects DeltaCam.

- [5] Tsai-Shien Chen, Chieh Hubert Lin, Hung-Yu Tseng, Tsung-Yi Lin, and Ming Yang. 2023. Motion-Conditioned Diffusion Model for Controllable Video Synthesis. *ArXiv abs/2304.14404* (2023). <https://api.semanticscholar.org/CorpusID:258352582>

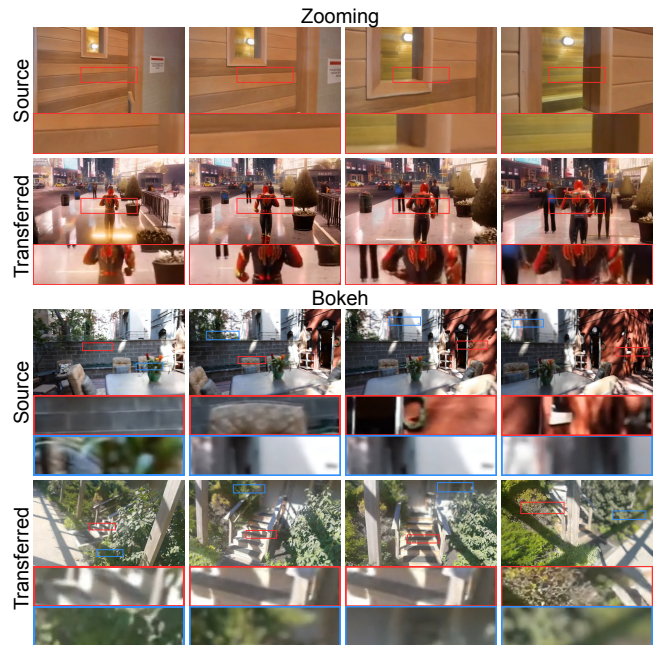


Fig. 14. Camera Style transfer. Video-to-video camera style transfer using style extraction and transfer to a new video. Zoomed insets indicate regions at similar depth or zooming direction.

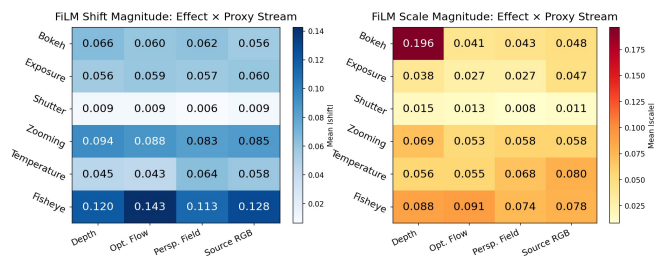


Fig. 15. Ablations. FiLM modulation strength by effect and proxy stream. Photometric effects rely on RGB; geometric effects rely on depth and perspective field.

- [6] I-Sheng Fang, Yue-Hua Han, and Jun-Cheng Chen. 2024. Camera settings as tokens: Modeling photography on latent diffusion models. In *SIGGRAPH Asia 2024 Conference Papers*. 1–11.
- [7] Daniel Geng, Charles Herrmann, Junhwa Hur, Forrester Cole, Serena Zhang, Tobias Pfaff, Tatiana Lopez-Guevara, Carl Doersch, Yusuf Aytar, Michael Rubinstein, Chen Sun, Oliver Wang, Andrew Owens, and Deqing Sun. 2024. Motion Prompting: Controlling Video Generation with Motion Trajectories. *2025 IEEE/CVF Conference on Computer Vision and Pattern Recognition (CVPR)* (2024), 1–12. <https://api.semanticscholar.org/CorpusID:274446282>
- [8] Yuchao Gu, Yipin Zhou, Bichen Wu, Licheng Yu, Jia-Wei Liu, Rui Zhao, Jay Zhangjie Wu, David Junhao Zhang, Mike Zheng Shou, and Kevin Tang. 2024. Videoswap: Customized video subject swapping with interactive semantic point correspondence. In *Proceedings of the IEEE/CVF Conference on Computer Vision and Pattern Recognition*. 7621–7630.
- [9] Zekai Gu, Rui Yan, Jiahao Lu, Peng Li, Zhiyang Dou, Chenyang Si, Zhen Dong, Qifeng Liu, Cheng Lin, Ziwei Liu, et al. 2025. Diffusion as shader: 3d-aware video diffusion for versatile video generation control. In *Proceedings of the Special Interest Group on Computer Graphics and Interactive Techniques Conference Conference Papers*. 1–12.
- [10] Pooja Guhan, Divya Kothandaraman, Tsung-Wei Huang, Guan-Ming Su, and Dinesh Manocha. 2025. CamMimic: Zero-Shot Image To Camera Motion Personalized Video Generation Using Diffusion Models. *arXiv preprint arXiv:2504.09472* (2025).
- [11] Yuliang Guo, Sparsh Garg, S Mahdi H Miangoleh, Xinyu Huang, and Liu Ren. 2025. Depth any camera: Zero-shot metric depth estimation from any camera. In *Proceedings of the Computer Vision and Pattern Recognition Conference*. 26996–27006.
- [12] Yoav HaCohen, Nisan Chiprut, Benny Brazowski, Daniel Shalem, David-Pur Moshe, Eitan Richardson, E. I. Levin, Guy Shiran, Nir Zabari, Ori Gordon, Poriya Panet, Sapir Weissbuch, Victor Kulikov, Yaki Bitterman, Zeev Melumian, and Ofir Bibi. 2024. LTX-Video: Realtime Video Latent Diffusion. *ArXiv abs/2501.00103* (2024). <https://api.semanticscholar.org/CorpusID:275212083>
- [13] Chen Hou and Zhibo Chen. 2024. Training-free camera control for video generation. *arXiv preprint arXiv:2406.10126* (2024).
- [14] Ziqi Huang, Yinan He, Jiashuo Yu, Fan Zhang, Chenyang Si, Yuming Jiang, Yuanhan Zhang, Tianxing Wu, Qingyang Jin, Nattapol Chanpaisit, Yaohui Wang, Xinyuan Chen, Limin Yang, Dahua Lin, Yu Qiao, and Ziwei Liu. 2023. VBench: Comprehensive Benchmark Suite for Video Generative Models. *2024 IEEE/CVF Conference on Computer Vision and Pattern Recognition (CVPR)* (2023), 21807–21818. <https://api.semanticscholar.org/CorpusID:265506207>
- [15] Zeyinzi Jiang, Zhen Han, Chaojie Mao, Jingfeng Zhang, Yulin Pan, and Yu Liu. 2025. Vace: All-in-one video creation and editing. In *Proceedings of the IEEE/CVF International Conference on Computer Vision*. 17191–17202.
- [16] Dongyoung Kim, Mahmoud Affif, Dongyun Kim, Michael S Brown, and Seon Joo Kim. 2025. CCMNet: Leveraging Calibrated Color Correction Matrices for Cross-Camera Color Constancy. *arXiv preprint arXiv:2504.07959* (2025).
- [17] Teng Li, Guangcong Zheng, Rui Jiang, Shuigen Zhan, Tao Wu, Yehao Lu, Yining Lin, Chuanyun Deng, Yapan Xiong, Min Chen, et al. 2025. Realcam-i2v: Real-world image-to-video generation with interactive complex camera control. In *Proceedings of the IEEE/CVF International Conference on Computer Vision*. 28785–28796.
- [18] Kang Liao, Size Wu, Zhonghua Wu, Linyi Jin, Chao Wang, Yikai Wang, Fei Wang, Wei Li, and Chen Chang Loy. 2025. Thinking with Camera: A Unified Multimodal Model for Camera-Centric Understanding and Generation. *arXiv preprint arXiv:2510.08673* (2025).
- [19] Chenlin Meng, Yutong He, Yang Song, Jiaming Song, Jiajun Wu, Jun-Yan Zhu, and Stefano Ermon. 2021. Sdedit: Guided image synthesis and editing with stochastic differential equations. *arXiv preprint arXiv:2108.01073* (2021).
- [20] Maxime Oquab, Timothée Darcet, Théo Moutakanni, Huy Vo, Marc Szafraniec, Vasil Khalidov, Pierre Fernandez, Daniel Haziza, Francisco Massa, Alaaeldin El-Nouby, et al. 2023. Dinov2: Learning robust visual features without supervision. *arXiv preprint arXiv:2304.07193* (2023).
- [21] Hao Ouyang, Zifan Shi, Chenyang Lei, Ka Lung Law, and Qifeng Chen. 2021. Neural camera simulators. In *Proceedings of the IEEE/CVF conference on computer vision and pattern recognition*. 7700–7709.
- [22] Ethan Perez, Florian Strub, Harm de Vries, Vincent Dumoulin, and Aaron C. Courville. 2017. FiLM: Visual Reasoning with a General Conditioning Layer. In *AAAI Conference on Artificial Intelligence*. <https://api.semanticscholar.org/CorpusID:19119291>
- [23] Alec Radford, Jong Wook Kim, Chris Hallacy, Aditya Ramesh, Gabriel Goh, Sandhini Agarwal, Girish Sastry, Amanda Askell, Pamela Mishkin, Jack Clark, et al. 2021. Learning transferable visual models from natural language supervision. In *International conference on machine learning*. PmlR, 8748–8763.
- [24] Mike Ranzinger, Greg Heinrich, Collin McCarthy, Jan Kautz, Andrew Tao, Bryan Catanzaro, and Pavlo Molchanov. 2026. C-RADIOv4 (Tech Report). *arXiv:2601.17237 [cs.CV]* <https://arxiv.org/abs/2601.17237>
- [25] Thomas Ressler-Antal, Frank Fundel, Malek Ben Alaya, Stefan Andreas Baumann, Felix Krause, Ming Gui, and Björn Ommer. 2025. DisMo: Disentangled Motion Representations for Open-World Motion Transfer. In *The Thirty-ninth Annual Conference on Neural Information Processing Systems*.
- [26] Tim Seizinger, Florin-Alexandru Vasluianu, Marcos V Conde, Zongwei Wu, and Radu Timofte. 2025. Bokehlicious: Photorealistic bokeh rendering with controllable apertures. In *Proceedings of the IEEE/CVF International Conference on Computer Vision*. 8908–8917.
- [27] Vincent Sitzmann, Semon Rezhchikov, Bill Freeman, Josh Tenenbaum, and Fredo Durand. 2021. Light field networks: Neural scene representations with single-evaluation rendering. *Advances in Neural Information Processing Systems* 34 (2021), 19313–19325.
- [28] Jiaming Song, Chenlin Meng, and Stefano Ermon. 2020. Denoising diffusion implicit models. *arXiv preprint arXiv:2010.02502* (2020).
- [29] SaiKiran Tedla, Kelly Zhu, Trevor Canham, Felix Taubner, Michael S Brown, Kiriakos N Kutulakos, and David B Lindell. 2025. Generating the Past, Present and Future from a Motion-Blurred Image. *ACM Transactions on Graphics (TOG)* 44, 6 (2025), 1–15.
- [30] Ang Wang, Baole Ai, Bin Wen, Chaojie Mao, Chen-Wei Xie, Di Chen, Fei Wu, Haiming Zhao, Jianxiao Yang, Jianyuan Zeng, Jiayu Wang, Jingfeng Zhang, Jingren Zhou, Jinkai Wang, Jixuan Chen, Kai Zhu, Kang Zhao, Keyu Yan, Lianghua Huang, Xiaofeng Meng, Ningying Zhang, Pandeng Li, Ping Wu, Ruihang Chu, Rui Feng, Shiwei Zhang, Siyang Sun, Tao Fang, Tianxing Wang, Tianyi Gui, Tingyu Weng, Tong Shen, Wei Lin, Wei Wang, Wei Wang, Wen-Chao Zhou, Wenten Wang, Wen Shen, Wenyuan Yu, Xianzhong Shi, Xiaomin Huang, Xin Xu, Yan Kou, Yan-Mei Lv, Yifei Li, Yijing Liu, Yiming Wang, Yingya Zhang, Yitong Huang, Yong Li, You Wu, Yu Liu, Yulin Pan, Yun Zheng, Yuntao Hong, Yupeng Shi, Yutong Feng, Zeyinzi Jiang, Zhengbin Han, Zhigang Wu, and Ziyu Liu. 2025. Wan: Open and Advanced Large-Scale Video Generative Models. *ArXiv abs/2503.20314* (2025). <https://api.semanticscholar.org/CorpusID:277321639>
- [31] Qinghe Wang, Yawen Luo, Xiaoyu Shi, Xu Jia, Huchuan Lu, Tianfan Xue, Xintao Wang, Pengfei Wan, Di Zhang, and Kun Gai. 2025. CineMaster: A 3D-Aware and Controllable Framework for Cinematic Text-to-Video Generation. *Proceedings of the Special Interest Group on Computer Graphics and Interactive Techniques Conference Conference Papers* (2025). <https://api.semanticscholar.org/CorpusID:276287673>
- [32] Xi Wang, Robin Courant, Marc Christie, and Vicky Kalogeiton. 2025. AKiRa: Augmentation Kit on Rays for optical video generation. In *Proceedings of the Computer Vision and Pattern Recognition Conference*. 2609–2619.
- [33] Yujie Wei, Shiwei Zhang, Zhiwu Qing, Hangjie Yuan, Zhiheng Liu, Yu Liu, Yingya Zhang, Jingren Zhou, and Hongming Shan. 2024. Dreamvideo: Composing your dream videos with customized subject and motion. In *Proceedings of the IEEE/CVF Conference on Computer Vision and Pattern Recognition*. 6537–6549.
- [34] Junfei Xiao, Ceyuan Yang, Lvmin Zhang, Shenggu Cai, Yang Zhao, Yuwei Guo, Gordon Wetzstein, Maneesh Agrawala, Alan Yuille, and Lu Jiang. 2025. Captain cinema: Towards short movie generation. *arXiv preprint arXiv:2507.18634* (2025).
- [35] Jinbo Xing, Long Mai, Cusuh Ham, Jiahui Huang, Aniruddha Mahapatra, Chi-Wing Fu, Tien-Tsin Wong, and Feng Liu. 2025. Motioncanvas: Cinematic shot design with controllable image-to-video generation. In *Proceedings of the Special Interest Group on Computer Graphics and Interactive Techniques Conference Conference Papers*. 1–11.
- [36] Zhuoyi Yang, Jiayan Teng, Wendi Zheng, Ming Ding, Shiyu Huang, Jiazheng Xu, Yuanming Yang, Wenyi Hong, Xiaohan Zhang, Shanyu Feng, et al. 2024. Cogvideox: Text-to-video diffusion models with an expert transformer. *arXiv preprint arXiv:2408.06072* (2024).
- [37] Wangbo Yu, Jinbo Xing, Li Yuan, Wenbo Hu, Xiaoyu Li, Zhipeng Huang, Xiangjun Gao, Tien-Tsin Wong, Ying Shan, and Yonghong Tian. 2024. Viewcrafter: Taming video diffusion models for high-fidelity novel view synthesis. *arXiv preprint arXiv:2409.02048* (2024).
- [38] Yu Yuan, Xijun Wang, Yichen Sheng, Prateek Chennuri, Xinguang Zhang, and Stanley Chan. 2025. Generative photography: Scene-consistent camera control for realistic text-to-image synthesis. In *Proceedings of the Computer Vision and Pattern Recognition Conference*. 7920–7930.
- [39] Lvmin Zhang, Anyi Rao, and Maneesh Agrawala. 2023. Adding conditional control to text-to-image diffusion models. In *Proceedings of the IEEE/CVF international conference on computer vision*. 3836–3847.
- [40] Yabo Zhang, Yuxiang Wei, Dongsheng Jiang, Xiaopeng Zhang, Wangmeng Zuo, and Qi Tian. 2023. ControlVideo: Training-free Controllable Text-to-Video Generation. *arXiv preprint arXiv:2305.13077* (2023).
- [41] Jensen Zhou, Hang Gao, Vikram Voleti, Aaryaman Vasishtha, Chun-Han Yao, Mark Boss, Philip Torr, Christian Rupprecht, and Varun Jampani. 2025. Stable virtual camera: Generative view synthesis with diffusion models. *arXiv preprint arXiv:2503.14489* (2025).
- [42] Zhenghong Zhou, Jie An, and Jiebo Luo. 2025. Latent-Reframe: Enabling Camera Control for Video Diffusion Models without Training. In *Proceedings of the IEEE/CVF International Conference on Computer Vision*. 12779–12789.